



PERGAMON

Available online at [www.sciencedirect.com](http://www.sciencedirect.com)

SCIENCE @ DIRECT®

International Journal of  
**Multiphase  
Flow**

International Journal of Multiphase Flow 29 (2003) 869–891

[www.elsevier.com/locate/ijmulflow](http://www.elsevier.com/locate/ijmulflow)

# A locally implicit improvement of the equilibrium Eulerian method

Jim Ferry <sup>a</sup>, Sarma L. Rani <sup>a</sup>, S. Balachandar <sup>b,\*</sup>

<sup>a</sup> Center for Simulation of Advanced Rockets, University of Illinois, Urbana-Champaign, IL, USA

<sup>b</sup> Department of Theoretical and Applied Mechanics, University of Illinois, 216 Talbot Laboratory, Urbana-Champaign, IL 61801, USA

Received 2 September 2002; received in revised form 30 March 2003

---

## Abstract

The equilibrium Eulerian method is a simple way to determine the velocity field of a disperse system of particles. It avoids solving a partial differential equation for particle velocity, which makes it more efficient than the standard Eulerian–Eulerian method. It captures such essential disperse-phase physics as preferential concentration and turbophoretic migration—effects which are ignored by methods that set the particle velocity equal to the fluid velocity. Although the equilibrium Eulerian method works well for small particles, it fails for particles that are too large. This paper presents a straightforward improvement to the method which minimizes the error for larger particles, thereby extending the method's range of applicability. In particular, it is demonstrated that the modified method captures a physical mechanism neglected by unmodified method: the memory a particle retains when it migrates to an adjacent layer of fluid. The improvement is demonstrated in a direct numerical simulation (DNS) of turbulent channel flow, where particles migrate toward the wall through a strong shear. It is also demonstrated that the modified method performs well in a case where no mean shear is present: a DNS of isotropic turbulence.

© 2003 Elsevier Science Ltd. All rights reserved.

*Keywords:* Two-phase flow; Eulerian; Equilibrium Eulerian; Fast Eulerian; Turbulent channel flow; Isotropic turbulence; Direct numerical simulation

---

## 1. Introduction

In the standard Eulerian–Eulerian method of evolving a multiphase flow, it is assumed that there is a unique particle velocity at every point in space. The derivation of the method obtains

---

\* Corresponding author. Tel.: +1-217-244-4371; fax: +1-217-244-9090.  
E-mail address: [s-bala@uiuc.edu](mailto:s-bala@uiuc.edu) (S. Balachandar).

this velocity by averaging over either an ensemble or a small volume, but the method can only work well when there is a narrow distribution of particle velocities at a given place and time. Ferry and Balachandar (2001) show that particles, in fact, entrain to a unique *equilibrium* velocity field provided their response time is sufficiently small compared to the time scales of the flow, under the assumption of one-way coupling. This result does more than validate the use of the Eulerian–Eulerian method: it suggests a new method wherein the particle velocity field  $\mathbf{v}$  is not obtained via the evolution of a partial differential equation (PDE), but is obtained directly from the local spatial and temporal derivatives of the fluid velocity field  $\mathbf{u}$ . This method was named the equilibrium Eulerian method (or fast Eulerian method). An example of its effectiveness at evolving concentration fields may be found in Ferry and Balachandar (2002).

Ferry and Balachandar (2001) evaluated the accuracy of a first-order approximation to the equilibrium Eulerian velocity by comparing ensembles of particles evolved with this velocity to those evolved with the exact velocity (obtained via Lagrangian tracking). Tests were performed in a turbulent channel flow of  $Re_\tau = 180$  for various particle-to-fluid density ratios and a wide range of nondimensional particle time scales. It was shown that for small particles of nondimensional time scale much less than unity the equilibrium Eulerian approach predicts the particle velocity accurately, and that as the particles increase in size the error correspondingly increases.

One of the most important physical effects captured accurately by the equilibrium Eulerian approximation is that of the mean migration of particles toward the wall. This is a feature of wall-bounded turbulent flows that has long been observed experimentally, beginning with Friedlander and Johnstone (1957). Explanations for this phenomenon were given independently by Camparaloni et al. (1975), and by Reeks (1983), who termed it *turbophoresis*, in analogy to the more familiar phenomenon of thermophoresis. The turbophoretic migration of particles toward walls has also been observed numerically (e.g., Kallio and Reeks, 1989; Brooke et al., 1994). The same phenomenon dictates that lighter-than-fluid bubbles migrate away from walls. The equilibrium Eulerian method accurately captures this turbophoretic wall-normal migration velocity for all particle-to-fluid density ratios ranging from dense particles to bubbles.

The equilibrium Eulerian method is, however, less successful in accurately capturing the streamwise particle velocity of larger particles. As will be shown (in Fig. 7b) there is a substantial discrepancy between the actual mean streamwise slip velocity and the value predicted by the equilibrium Eulerian method, for large particles close to the no-slip walls. For the largest particle considered ( $\tau^+ = 3$ ) in the high shear region close to the walls the actual streamwise slip velocity and the corresponding prediction by the equilibrium Eulerian method are 0.18 and 0.08, respectively. This discrepancy arises due to the approximation of  $\mathbf{v} \cdot \nabla \mathbf{v}$  by  $\mathbf{u} \cdot \nabla \mathbf{u}$  in the equilibrium Eulerian approach. In particular, the discrepancy in the streamwise slip arises from the difference between  $v_2 \partial v_1 / \partial y$  and  $u_2 \partial u_1 / \partial y$ . In the near-wall region the fluid and particle shear are comparable (at  $y^+ = 7$ :  $\partial v_1 / \partial y \approx \partial u_1 / \partial y \approx 0.8$ ). However, the mean wall-normal velocity of the particles is different from that of the fluid due to turbophoretic migration. For example, for the largest particle considered ( $\tau^+ = 3$ ) in the near-wall region the difference reaches a peak of  $\langle v_2 - u_2 \rangle = 0.04$ . Although this turbophoretic migration velocity might appear much smaller than the mean streamwise velocity, in combination with the strong near-wall shear it can lead to a substantial error in the equilibrium estimation of the near-wall streamwise velocity (this discrepancy being approximately  $\tau^+(v_2 - u_2)\partial u_1 / \partial y$ ). In essence, as particles migrate across fluid streamlines, their velocity differs from the local fluid velocity due to the finite memory the inertial

particles retain of where they came from. The equilibrium Eulerian approximation fails to account for this mechanism at  $O(\tau)$  and hence results in the observed discrepancy in the streamwise slip in the turbulent channel flow.

Here we propose a simple modification to the equilibrium Eulerian approach, which accounts for the effect of the transverse motion of particles across fluid streamlines on the particles' streamwise velocity. One possible approach is to systematically extend the equilibrium Eulerian expansion to include all terms of  $O(\tau^2)$ , as it can be expected that the higher-order effect of momentum carried by the particles across streamlines to appear at this level. However, these higher-order terms are poorly behaved, from a computational perspective, since they involve even higher order derivatives of the form  $D^2\mathbf{u}/Dt^2$ . Furthermore, it has been observed in Ferry and Balachandar (2001) that with the inclusion of all the  $O(\tau^2)$  terms the predictive capability of the equilibrium approximation degrades for all but the smallest particles. Instead, in Section 2 we derive a modified equilibrium Eulerian method based on some simple heuristic assumptions and show that it incorporates certain important  $O(\tau^2)$  terms. This modification also introduces some implicitness in the approximation of the equilibrium particle velocity field. The remainder of the paper evaluates the effect of this local implicitness on the predictive capability of particle velocity by comparing the modified equilibrium velocity with the original (unmodified) one presented in Ferry and Balachandar (2001) and with the exact Lagrangian particle velocity. Section 3 explores the behavior of these different methods analytically for simple linearly varying ambient flows. These simple results will prove quite useful in explaining the equilibrium Eulerian velocities obtained in the more complex cases of isotropic turbulence and turbulent channel flow to be discussed in Sections 4 and 5. Conclusions are drawn in Section 6.

## 2. Locally implicit equilibrium particle velocity

For the simple case of a particle acted on by Stokes drag and gravity, the equation for the particle velocity  $\mathbf{v}$  is

$$\frac{d\mathbf{v}}{dt} = \frac{\mathbf{u} - \mathbf{v}}{\tau} + \mathbf{g}. \tag{1}$$

If  $\tau$  is sufficiently small, then it is appropriate to express  $\mathbf{v}$  as an expansion in terms of  $\mathbf{u}$ , with  $\tau$  as the small parameter. Such an expansion can be used to substitute for  $d\mathbf{v}/dt$  in (1), and after re-arrangement one obtains the expansion (Ferry and Balachandar, 2001):

$$\mathbf{v} - \mathbf{u} = -\tau \left( \frac{D\mathbf{u}}{Dt} - \mathbf{g} \right) + O(\tau^2). \tag{2}$$

The equilibrium Eulerian method approximates  $\mathbf{v}$  by its first-order expansion in  $\tau$ :

$$\mathbf{v}_e = \mathbf{u} - \tau \left( \frac{D\mathbf{u}}{Dt} - \mathbf{g} \right). \tag{3}$$

This method of determining the particle velocity is intermediate in complexity between evolving a PDE to find  $\mathbf{v}$  (the standard Eulerian method) and simply setting  $\mathbf{v} = \mathbf{u}$ , as is done in the dusty gas method (Saffman, 1962; Marble, 1970) or  $\mathbf{v} = \mathbf{u} + \tau\mathbf{g}$  (Manninen et al., 1996). The relative

importance of gravitational settling in the above equations is determined by the ratio of gravitational acceleration to local fluid acceleration ( $|\mathbf{g}|/|\mathbf{D}\mathbf{u}/\mathbf{D}t|$ ). For values of this ratio much less than unity the effect of gravity can be neglected and for the case  $|\mathbf{g}| \approx |\mathbf{D}\mathbf{u}/\mathbf{D}t|$  the effects of both local fluid and gravitational acceleration contribute to particle slip. For the case of very strong settling ( $|\mathbf{g}| \gg |\mathbf{D}\mathbf{u}/\mathbf{D}t|$ ), to the leading order the equilibrium approximation reduces to the dusty gas formalism.

The important advantage of the equilibrium Eulerian approximation is that it is computationally very efficient. This applies especially when particles of various sizes are evolved, because this requires a particle velocity field for each size to be solved in the standard case, whereas in the equilibrium approximation, once the  $O(\tau)$  correction is evaluated the velocity field of the different particle sizes can be readily obtained. The other advantage is that it avoids the computational difficulties of the standard Eulerian approach associated with evolving the particulate momentum equation for  $\mathbf{v}$ , especially in the limit of small particle response time  $\tau$ .

Though simpler than the standard method, the equilibrium Eulerian method is more costly and complicated than simply setting  $\mathbf{v} = \mathbf{u} + \tau\mathbf{g}$ . However, using such an approximation implies that an initially uniform particle field will stay uniform, in contradiction to the observed phenomena of preferential concentration (Maxey, 1987; Squires and Eaton, 1991; Eaton and Fessler, 1994) and turbophoretic migration. So if  $\mathbf{v} = \mathbf{u} + \tau\mathbf{g}$  is to be used, the particles must be small enough that these effects are very weak. On the other hand, the equilibrium Eulerian approach captures these effects accurately, reproducing the exact analytic behavior to  $O(\tau)$  accuracy.

Comparing (1) and (3) shows that the equilibrium Eulerian method can be described as simply modeling  $d\mathbf{v}/dt$  by  $\mathbf{D}\mathbf{u}/\mathbf{D}t$ . Although this closure works quite well when  $\tau$  is small, when  $\tau$  becomes sufficiently large, the error in the approximation becomes significant. In a direct numerical simulation (DNS) of turbulent channel flow, it was observed that with increasing  $\tau$ , the first statistic to develop an error is the streamwise slip velocity. Heavier-than-fluid particles on average migrate toward the walls, and therefore in the near-wall region they tend to move faster along the streamwise direction than the slow-moving near-wall fluid. In contrast, lighter-than-fluid particles migrate away from the wall and therefore their streamwise velocity lags the local fluid velocity. This streamwise slip velocity of particles is underestimated with the equilibrium Eulerian approximation (3).

The reason for this underestimation is that the equilibrium Eulerian method fails to represent the wall-normal transport of streamwise velocity due to the turbophoretic migration of particles. Because  $\mathbf{v}$  has a wallward component significantly different than  $\mathbf{u}$ , the  $\mathbf{u} \cdot \nabla\mathbf{u}$  term in  $\mathbf{D}\mathbf{u}/\mathbf{D}t$  provides a poor approximation to  $\mathbf{v} \cdot \nabla\mathbf{v}$  in  $d\mathbf{v}/dt$ . The approximation can be improved if instead of the closure  $d\mathbf{v}/dt \approx \mathbf{D}\mathbf{u}/\mathbf{D}t$  one uses  $d\mathbf{v}/dt \approx d\mathbf{u}/dt$ :

$$\mathbf{v} - \mathbf{u} = -\tau \left( \frac{\mathbf{D}\mathbf{u}}{\mathbf{D}t} + \mathbf{G}(\mathbf{v} - \mathbf{u}) - \mathbf{g} \right), \quad (4)$$

where  $\mathbf{G} = (\nabla\mathbf{u})^T$ . This might be considered an implicit equation for  $\mathbf{v} - \mathbf{u}$ , but it only requires a  $3 \times 3$  matrix to be inverted locally at every point for the evaluation of the local equilibrium particle velocity. Collecting the terms of (4) involving  $\mathbf{v} - \mathbf{u}$  yields the following improved equilibrium approximation:

$$\mathbf{v}_m = \mathbf{u} - \tau(\mathbf{I} + \tau\mathbf{G})^{-1} \left( \frac{D\mathbf{u}}{Dt} - \mathbf{g} \right). \tag{5}$$

The only difference between (3) and (5) is the correction factor  $(\mathbf{I} + \tau\mathbf{G})^{-1}$ . The former will be referred to as the unmodified equilibrium approximation, and the latter as the modified equilibrium approximation. The equilibrium and modified equilibrium approximations agree to first order ( $\mathbf{v}_e - \mathbf{v}_m = O(\tau^2)$ ), so all the first-order results about the unmodified equilibrium Eulerian method carry over to the modified method: e.g., turbophoretic migration, preferential concentration. However, the modified method shows some nice features when we investigate the precise form of this error. Let  $\mathbf{v}$  denote the exact solution to (1), and  $d/dt$ , a derivative following the exact solution. Then

$$\begin{aligned} \mathbf{v}_e - \mathbf{v} &= \tau \left( (\mathbf{v} - \mathbf{u}) \cdot \nabla \mathbf{u} + \frac{d}{dt} (\mathbf{v} - \mathbf{u}) \right), \\ \mathbf{v}_m - \mathbf{v} &= \tau \left( (\mathbf{v} - \mathbf{v}_m) \cdot \nabla \mathbf{u} + \frac{d}{dt} (\mathbf{v} - \mathbf{u}) \right). \end{aligned} \tag{6}$$

These equations split the error into two components: that due to migration of particles through a velocity gradient, and due to rate of change of slip velocity along a particle path. The first term can make  $\mathbf{v}_e - \mathbf{v}$  relatively large when a particle migrates (via turbophoresis or gravity) through a shear flow. Note, however, that this term becomes much smaller for  $\mathbf{v}_m - \mathbf{v}$  because  $|\mathbf{v} - \mathbf{v}_m| \ll |\mathbf{v} - \mathbf{u}|$ .

Expanding (5) in  $\tau$  yields

$$\mathbf{v}_m = \mathbf{u} - \tau \left( \frac{D\mathbf{u}}{Dt} - \mathbf{g} \right) + \tau^2 \mathbf{G} \left( \frac{D\mathbf{u}}{Dt} - \mathbf{g} \right) + O(\tau^3). \tag{7}$$

This may be compared to the following exact power series expansion for  $\mathbf{v}$ , which can be obtained directly from (1):

$$\mathbf{v} = \mathbf{u} - \tau \left( \frac{D\mathbf{u}}{Dt} - \mathbf{g} \right) + \tau^2 \left( \mathbf{G} \left( \frac{D\mathbf{u}}{Dt} - \mathbf{g} \right) + \frac{D^2\mathbf{u}}{Dt^2} \right) + O(\tau^3). \tag{8}$$

Note that the  $O(\tau^2)$  term in the modified equilibrium approximation ( $\mathbf{v}_m$ ) agrees with only the part of the  $O(\tau^2)$  term in the exact expansion ( $\mathbf{v}$ ) that represents migration through a velocity gradient. It was observed in Ferry and Balachandar (2001) that the inclusion of the entire  $O(\tau^2)$  term, as given in the exact expansion (8), does not significantly improve the accuracy of the equilibrium velocity estimate. In fact, for large particles the error increases with the inclusion of the  $O(\tau^2)$  term. Part of the reason for this is the poor computational behavior of  $D^2\mathbf{u}/Dt^2$ , which involves higher-order derivatives. In addition, the standard equilibrium approximations truncated to  $O(\tau)$  or  $O(\tau^2)$  continue to worsen in an unbounded manner as  $\tau$  increases. The implicit nature of the modified method, however, alleviates the problem: as  $\tau \rightarrow \infty$ ,  $\mathbf{v}_m$  approaches a constant, and the error, although it may be substantial, remains bounded.

### 3. Steady linear ambient flows

Here we will consider simple cases of steady linear ambient flows of the form

$$\mathbf{u} = \mathbf{G}\mathbf{x}, \quad (9)$$

where the velocity gradient matrix  $\mathbf{G}$  is constant. In such simple ambient flows, it is easy to solve (1) to obtain the exact particle velocity. It is also easy to determine the trajectories of particles evolved with either the modified or the unmodified equilibrium Eulerian velocity. We shall consider the three cases of a particle settling through a linear shear flow, a particle in a vortex, and a particle in an extensional or compressive straining flow.

#### 3.1. Particle settling in linear shear flow

A linear shear flow is given by  $\mathbf{u}(\mathbf{x}, t) = kx_2\hat{\mathbf{e}}_1$ , and a settling velocity by  $\mathbf{w} = -w\hat{\mathbf{e}}_2$  (where  $w = \tau g$ ). For this flow  $D\mathbf{u}/Dt = 0$ , so

$$\mathbf{v}_e = \mathbf{u} + \mathbf{w} \quad \text{and} \quad \mathbf{v}_m = \mathbf{u} + (\mathbf{I} + \tau\mathbf{G})^{-1}\mathbf{w}. \quad (10)$$

Because  $(\mathbf{I} + \tau\mathbf{G})^{-1}\mathbf{w} = k\omega\tau\hat{\mathbf{e}}_1 - w\hat{\mathbf{e}}_2$ , the difference between  $\mathbf{v}_e$  and  $\mathbf{v}_m$  is constant, and is in the streamwise direction. We now solve (1) to get the exact particle velocity. Re-writing (1) (with  $\mathbf{u} = \mathbf{G}\mathbf{x}$ ) in terms of  $\mathbf{x}$  and  $\mathbf{w}$ , gives  $\tau\ddot{\mathbf{x}} + \dot{\mathbf{x}} - \mathbf{G}\mathbf{x} = \mathbf{w}$ , which can be solved along with the initial conditions to obtain:

$$\begin{aligned} x_1(t) &= x_1(0) + kt(x_2(0) + w\tau + 2\tau(v_2(0) + w)) - k\omega t^2/2 \\ &\quad + \tau(v_1(0) - k(x_2(0) + w\tau + (t + 2\tau)(v_2(0) + w)))(1 - \exp(-t/\tau)), \\ x_2(t) &= x_2(0) - wt - \tau(v_2(0) + w)(1 - \exp(-t/\tau)). \end{aligned} \quad (11)$$

After the transients decay, we obtain the following expressions for the fluid velocity (at the particle location) and the particle velocity:

$$\begin{aligned} u_1(t) &= k(x_2(0) + \tau(v_2(0) + w) - wt), & u_2(t) &= 0, \\ v_1(t) &= k(x_2(0) + \tau(v_2(0) + 2w) - wt), & v_2(t) &= -w. \end{aligned} \quad (12)$$

Therefore the settling velocity is indeed  $-w$ , as predicted by both the modified and unmodified Eulerian methods. The exact streamwise velocity can be expressed as  $v_1(t) = u_1(t) + k\omega\tau$ . This is precisely what was predicted by the modified equilibrium Eulerian method. The streamwise slip velocity,  $k\omega\tau$ , represents the memory a particle retains of faster streamwise motion at a distance  $w\tau$  above its current position.

The simple shear flow example models the turbulent channel flow problem, with gravitational settling serving as a proxy for turbophoretic velocity. The example suggests that the local implicitness will fix the problem of streamwise lag, and in Section 5 it is shown that this is indeed the case. Accurate prediction of streamwise slip may be important in the case of the two-way coupled formulation because of its impact on the wallward transport of streamwise momentum.

### 3.2. Particle in a vortex

Here we consider the case of a particle in a vortex and ignore the effect of gravity. It is convenient to work with complex numbers rather than real vectors. Let  $z = x + iy$  denote the particle position,  $v = \dot{z}$  be the particle velocity, and  $u = ikz$  (with  $k$  real and positive) be the fluid velocity. The equation of motion of the particle reduces to

$$\tau \ddot{z} + \dot{z} - ikz = 0. \tag{13}$$

The roots of this ODE's characteristic equation are

$$r_{\pm} = \frac{-1 \pm \sqrt{1 + 4i\tau k}}{2\tau}. \tag{14}$$

Therefore the solutions for  $z$  and  $v$  have the form

$$z(t) = c_+ e^{r_+ t} + c_- e^{r_- t} \quad \text{and} \quad v(t) = c_+ r_+ e^{r_+ t} + c_- r_- e^{r_- t}. \tag{15}$$

$\text{Re}(r_+)$  is guaranteed to be greater than zero, which implies the physically obvious fact that particles are spun out of vortices. Furthermore, because  $\text{Re}(r_-) < \text{Re}(r_+)$ , the root  $r_-$  always represents a faster decay than  $r_+$ , and can be ignored as a transient (and, in fact,  $\text{Re}(r_-) < -1/\tau$ , so the transient decays rapidly). Therefore we have the result

$$v(t) = r_+ z(t) = \omega kz(t), \tag{16}$$

where  $\omega$  is a dimensionless measure of the particle velocity as a function of position.

Similarly, we can define  $\omega_0 = v_0/kz$ ,  $\omega_e = v_e/kz$ , and  $\omega_m = v_m/kz$  to be related to the different approximations  $\mathbf{v}$  the fluid, equilibrium Eulerian, and modified equilibrium Eulerian velocity, respectively. The results can be written in terms of the non-dimensional parameter  $\eta = k\tau$ , which expresses the strength of the vortical flow relative to the particle response time:

$$\begin{aligned} \omega_0 &= i, & \omega_m &= i + \frac{\eta}{1 + i\eta} = \frac{i}{1 + i\eta}, \\ \omega_e &= i + \eta, & \omega &= \frac{-1 + \sqrt{1 + 4i\eta}}{2\eta} = \frac{2i}{1 + \sqrt{1 + 4i\eta}}. \end{aligned} \tag{17}$$

Let us first investigate their behaviors in the small- and large- $\eta$  limits. The Taylor series about  $\eta = 0$  in each case are

$$\begin{aligned} \omega_0 &= i, & \omega_m &= i + \eta - i\eta^2 - \eta^3 + O(\eta^4), \\ \omega_e &= i + \eta, & \omega &= i + \eta - 2i\eta^2 - 5\eta^3 + O(\eta^4). \end{aligned} \tag{18}$$

Unlike in the shear flow, the locally implicit correction does not yield a solution of higher-order accuracy. The correction does however reduce the error by 50% for small  $\eta$ . Although the

equilibrium methods are intended for only small  $\tau$ , it is interesting to observe their behavior in the limit  $\eta \rightarrow \infty$ . The Taylor series in  $\zeta = \eta^{-1}$  about  $\zeta = 0$  are

$$\begin{aligned} \omega_0 &= i, & \omega_m &= \zeta + i\zeta^2 + O(\zeta^3), \\ \omega_e &= \zeta^{-1} + i, & \omega &= \frac{1+i}{\sqrt{2}}\zeta^{1/2} - \frac{1}{2}\zeta + \frac{1-i}{8\sqrt{2}}\zeta^{3/2} + O(\zeta^{5/2}). \end{aligned} \tag{19}$$

For large  $\eta$  the unmodified equilibrium Eulerian method is worse than any other method, whereas  $\omega_m \rightarrow 0$ , just as  $\omega \rightarrow 0$ , albeit at a different rate.

The real part of  $\omega$  (shown in Fig. 1a) corresponds to the radial particle velocity and has the important role of governing the preferential concentration of particles. The  $\mathbf{v} = \mathbf{u}$  approximation completely ignores the radial migration of the particle, whereas the equilibrium Eulerian method captures the effect well for small  $\eta$ . Unfortunately, the equilibrium Eulerian method extrapolates this small- $\eta$  behavior to all  $\eta$ , whereas in reality, sufficiently large particles cease to be spun out at all, because  $\text{Re}(\omega) \rightarrow 0$  for  $\eta \rightarrow \infty$ . A closer examination of Fig. 1a indicates that  $\text{Re}(\omega)$  reaches a peak value of 0.3003 at  $\eta = 1.029$  and further decay of  $\text{Re}(\omega)$  is very slow. The behavior of  $\text{Re}(\omega_m)$  is qualitatively correct: it increases first, reaches a maximum value of 0.5 at  $\eta = 1$  and then decays slowly to zero for large  $\eta$ .

As a dense particle is spun out radially it retains its lower azimuthal velocity as it encounters an ambient flow of higher azimuthal velocity. Fig. 1b illustrates that both the  $\mathbf{v} = \mathbf{u}$  and the unmodified equilibrium Eulerian method ignore this effect. The modified equilibrium Eulerian method captures this azimuthal slip reasonably for  $\eta \lesssim 0.8$ . For larger  $\eta$  the departure from the true behavior increases. The azimuthal slip here plays the role that streamwise slip plays in the shear flow case, and could be important in terms of the vortex-induced lift force and the impact of particles on angular momentum balance in the case of two-way coupling.

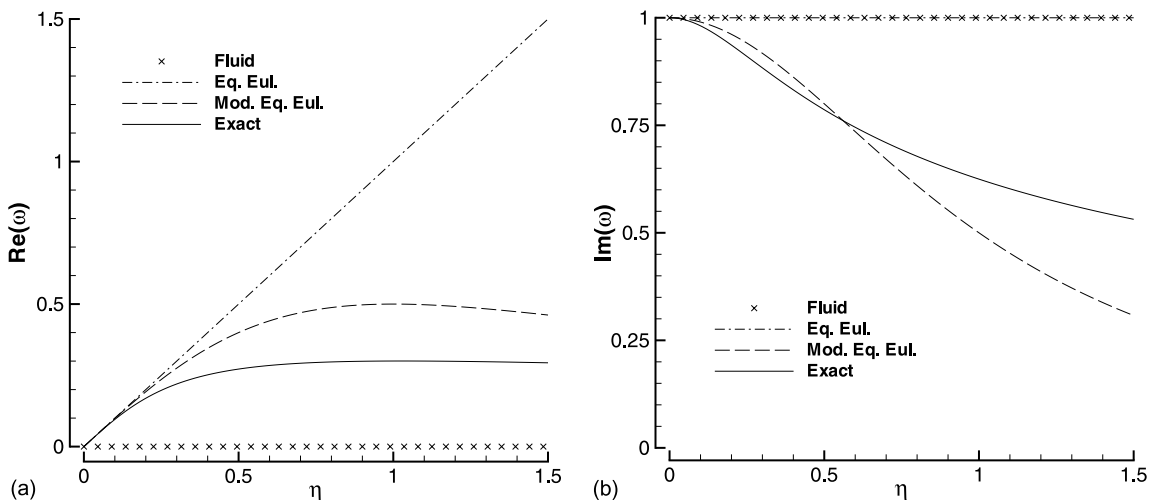


Fig. 1. (a) Radial and (b) azimuthal velocity factors for vortical flow.



3.3. Particle in extensional or compressive strain

For extensional strain, let  $u = kx$ , with  $k > 0$ . Then the particle velocity can be expressed as  $v = \omega kx$ , where, as in the vortex case, the transient is ignored for the exact solution. The exact and the approximate solutions along with their Taylor series expansions are given below (see Fig. 2a):

$$\begin{aligned} \omega_0 &= 1, & \omega_m &= \frac{1}{1 + \eta} = 1 - \eta + \eta^2 + O(\eta^3), \\ \omega_e &= 1 - \eta, & \omega &= \frac{-1 + \sqrt{1 + 4\eta}}{2\eta} = 1 - \eta + 2\eta^2 + O(\eta^3). \end{aligned} \tag{20}$$

The modified equilibrium Eulerian solution is much closer to the exact solution over the entire range of  $\eta$ .

For compressive strain, let  $u = -kx$ , with  $k > 0$ . The  $\omega$ -values are the same as in the extensional case, with  $\eta$  replaced by  $-\eta$ :

$$\begin{aligned} \omega_0 &= 1, & \omega_m &= \frac{1}{1 - \eta} = 1 + \eta + \eta^2 + O(\eta^3), \\ \omega_e &= 1 + \eta, & \omega &= \frac{-1 + \sqrt{1 - 4\eta}}{2\eta} = 1 + \eta + 2\eta^2 + O(\eta^3). \end{aligned} \tag{21}$$

Note that the exact solution,  $\omega$ , given above is valid only for  $\eta < 1/4$ . For  $\eta \geq 1/4$  the roots of the characteristic equation have the same real part, in which case it is impossible to separate the solution into dominant and transient parts. Physically, for  $\eta \geq 1/4$  the particle's inertia is too strong for it to approach the origin monotonically. Instead, the particle overshoots the origin and executes an oscillatory motion. As a result, the velocity field cannot be expressed as a unique function of its position. Several different branches of the exact solution are shown in Fig. 2b. Also note that  $\omega_m$  becomes singular at  $\eta = 1$ . However, it is clear that over the range  $0 \leq \eta \leq 1/4$ , the

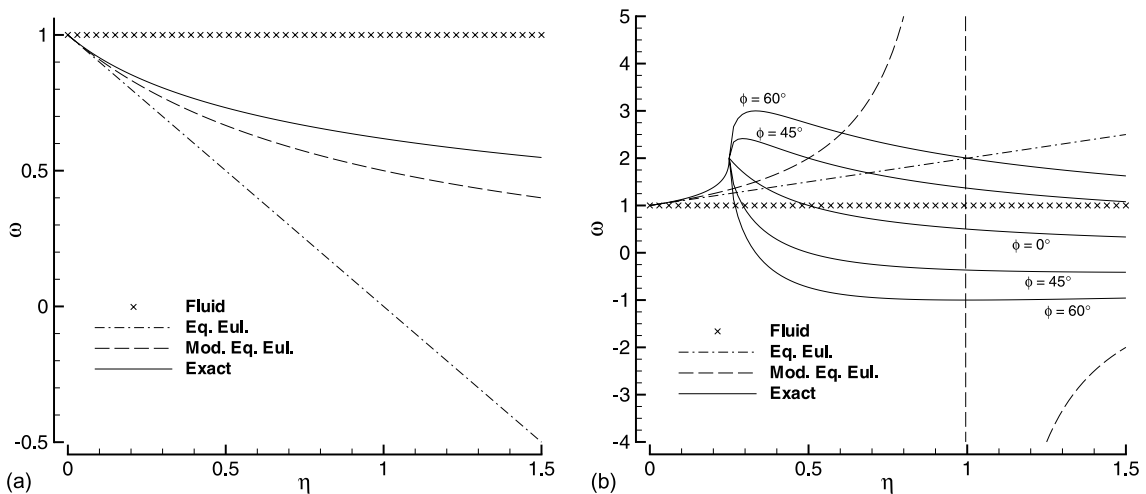


Fig. 2. Velocity factors for (a) extensional and (b) compressive strain.

locally implicit correction improves the solution over the unmodified equilibrium Eulerian approach.

### 3.4. Summary of examples

The motivation for the modified equilibrium Eulerian method was to eliminate errors associated with the streamwise momentum carried by a particle as it migrates across fluid streamlines. In the cases of shear and vortical flow, the unmodified method fails to account for the changing flow conditions seen by the particle, whereas the modified method accounts for the effect.

The impact of the different approximations on the preferential concentration of particles can be evaluated as well. The vortex and straining flow cases can be examined by comparing  $\omega_m$  and  $\omega$  in (18) with the corresponding values in (20) (or (21)). For small  $\eta$ , the radial migration of particles in the vortex,  $\text{Re}(\omega)$ , as predicted by the unmodified and modified methods are in agreement with the exact result at order  $\eta^2$ , while in the straining flows the prediction of entrainment is accurate only to order  $\eta$ . However, the modified method reduces the leading order error in preferential concentration by a factor of 2 in the case of straining flows, but only by 20% in the case of a vortex.

Along the direction of compressional strain, for  $\eta > 1/4$ , a unique particle velocity is not possible—the long time oscillatory behavior of the particle remains influenced by its initial condition. Thus an equilibrium Eulerian velocity for the particles under such a condition needs to be interpreted with caution. For lack of precise information on the initial distribution of all particles in a typical multiphase flow, one may simply consider the equilibrium Eulerian velocity to approximate the average behavior (instead of the unique motion) of the particles under such a condition of strong compressional strain. The modified equilibrium approximation faces difficulty as  $\eta$  approaches unity, as the implicit operator becomes singular. However, it must be emphasized that the equilibrium Eulerian method is intended only for particles in flow conditions such that  $\eta$  is small. Nevertheless, in Appendix A we present a simple algorithm which for small  $\eta$  reduces to the modified method but as  $\eta \rightarrow 1$  avoids the singularity.

## 4. Numerical study: isotropic turbulence

In our first numerical study we consider particle motion in isotropic turbulence and evaluate the accuracy of the unmodified and modified equilibrium approaches by comparing their statistics with those obtained from the exact particle motion. In isotropic turbulence, there is neither a wall layer, nor any associated turbophoretic migration, nor a mean streamwise slip velocity. Therefore, we will focus attention on different measures of preferential concentration of particles.

A DNS of forced isotropic turbulence data is performed using a Fourier pseudospectral method (Eswaran and Pope, 1988a,b). The flow domain consists of a cubic box of length  $L = 2\pi$  discretized into  $96^3$  equispaced grid points, with periodic boundary conditions in all three directions. The results to be reported are for a Taylor microscale Reynolds number  $Re_\lambda (= u' \lambda / \nu)$  of 60.5. Six different ensembles of 100,000 particles each with response times  $\tau^k = 0.08, 0.16, 0.32, 0.64, 1.28,$  and  $2.56$ , are evolved using the exact, equilibrium Eulerian, and modified equilibrium Eulerian velocities, yielding 18 different data sets. The gravitational acceleration is zero in each case. The

response time  $\tau^k$  and all other quantities to be presented in this section have been nondimensionalized by the Kolmogorov scale. The interpolation of fluid velocity to particle location was accomplished using the first derivative method, which is defined in Appendix B. Particles were evolved for 15,000 time steps to reach a statistically stationary state, which corresponds to at least 20 particle response times, and then statistics were gathered for another 15,000 time steps. The exact Lagrangian particle velocities and positions were obtained by fourth-order Adams–Bashforth and Adams–Moulton schemes, respectively.

Here we examine two different measures of preferential concentration:  $|\mathbf{S}|^2 - |\mathbf{\Omega}|^2$  and the swirling strength  $\lambda_i$ . The former is motivated by the analytical estimation of preferential concentration obtained by Maxey (1987) as

$$\nabla \cdot \mathbf{v} = -\tau \left( |\mathbf{S}|^2 - |\mathbf{\Omega}|^2 \right) + \mathcal{O}(\tau^2), \tag{22}$$

where  $\mathbf{S}$  and  $\mathbf{\Omega}$  are the symmetric and antisymmetric parts of  $\nabla \mathbf{u}$ , respectively. The latter is defined to be magnitude of the imaginary part of the pair of complex conjugate eigenvalues of the fluid velocity gradient  $\nabla \mathbf{u}$ . If all eigenvalues are real, then  $\lambda_i$  is defined to be zero. The swirling strength is a geometrically motivated indicator of the presence of vortical structures (Zhou et al., 1996). It is a more relevant measure of vortical structure than the magnitude of the vorticity: for example, it deems shear flow nonvortical.

In Fig. 3, the ensemble averaged quantities  $\langle |\mathbf{S}|^2 - |\mathbf{\Omega}|^2 \rangle$  and  $\langle \lambda_i \rangle$  are plotted versus  $\tau^k$ . The average is taken over all particles in an ensemble and over time. It is observed that both the unmodified and modified equilibrium Eulerian schemes compare well with the exact statistics (of the Lagrangian particles) for  $\tau^k \lesssim 0.32$ . For  $\tau^k \gtrsim 0.32$  there is an increasing discrepancy between the approximations and the exact result in both plots. The peak preferential concentration for the exact particles, as indicated by both  $\langle |\mathbf{S}|^2 - |\mathbf{\Omega}|^2 \rangle$  and  $\lambda_i$ , occurs for  $\tau^k = 0.64$ . As  $\tau^k$  increases further, the value of  $\langle |\mathbf{S}|^2 - |\mathbf{\Omega}|^2 \rangle$  for the exact particles decreases, in agreement with the expectation that for very large particles there will be little preferential concentration. This agrees with

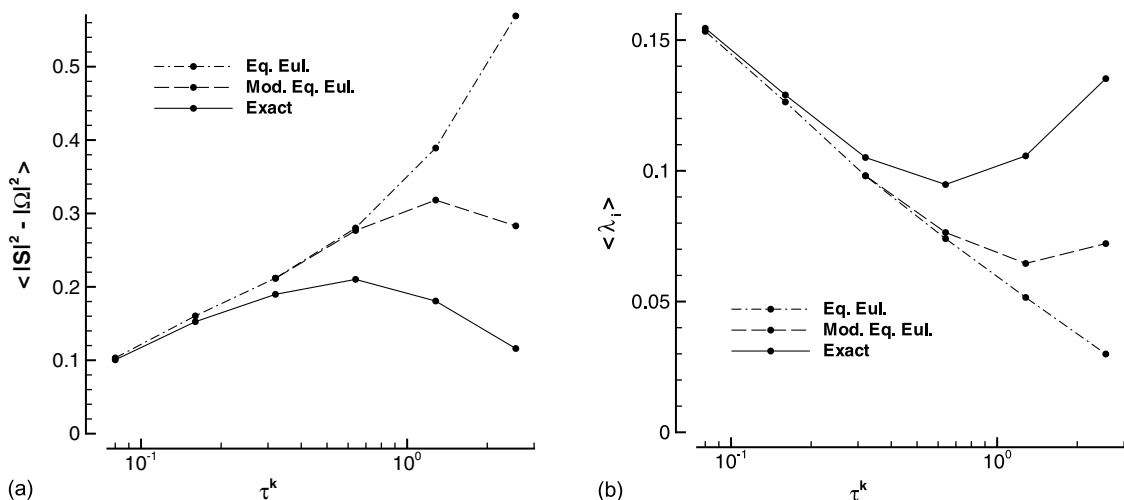


Fig. 3. Mean statistics as a function of  $\tau^k$ : (a)  $\langle |\mathbf{S}|^2 - |\mathbf{\Omega}|^2 \rangle$  and (b)  $\langle \lambda_i \rangle$ .

the earlier observation (Eaton and Fessler, 1994) that preferential concentration is most effective when the time scale of the particle approximately matches that of the Kolmogorov eddies. The unmodified equilibrium Eulerian method exhibits a monotonic increase in  $\langle |\mathbf{S}|^2 - |\boldsymbol{\Omega}|^2 \rangle$  with  $\tau^k$ , and hence an unphysical, ever-increasing preferential accumulation. The modified equilibrium approximation arrests this trend and exhibits a maximum value of  $\langle |\mathbf{S}|^2 - |\boldsymbol{\Omega}|^2 \rangle$  for  $\tau^k \approx 1$ , and a further decrease in preferential concentration for larger particles. The behavior of the  $\lambda_i$  statistics is similar.

Figs. 4 and 5 show the PDFs of  $|\mathbf{S}|^2 - |\boldsymbol{\Omega}|^2$  and  $\lambda_i$  for particles of size  $\tau^k = 0.32$  and 1.28. The PDFs for the exact, modified, and unmodified equilibrium particles are shown, as well as the PDF based on fluid statistics at the grid points. It is clear from the figures that the locally implicit

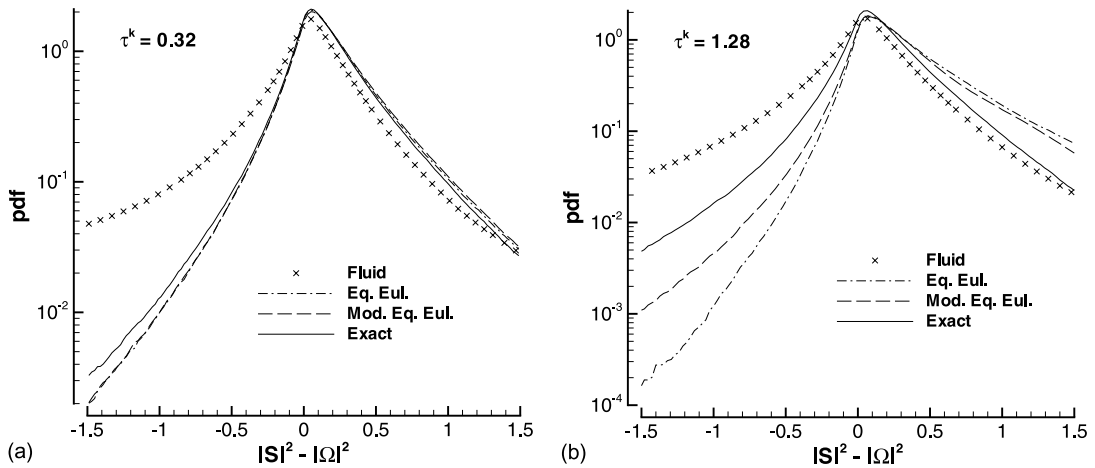


Fig. 4. Probability distribution function of  $|\mathbf{S}|^2 - |\boldsymbol{\Omega}|^2$ : (a)  $\tau^k = 0.32$  and (b)  $\tau^k = 1.28$ .

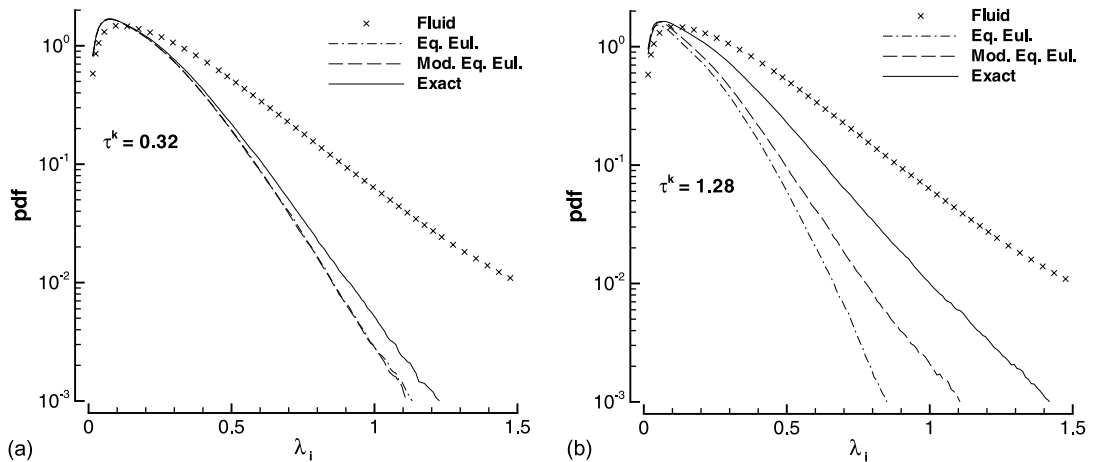


Fig. 5. Probability distribution function of  $\lambda_i$ : (a)  $\tau^k = 0.32$  and (b)  $\tau^k = 1.28$ .

correction does not have a significant influence on the statistics for small particles. However, for the larger particles of  $\tau^k = 1.28$  the locally implicit correction does provide some improvement.

## 5. Numerical study: turbulent channel flow

### 5.1. Description of the simulation

In our other numerical study a DNS of a turbulent flow is performed in a channel with dimensions  $4\pi h$  in the streamwise ( $x$ ),  $2h$  in the wall-normal ( $y$ ), and  $4\pi h/3$  in the spanwise ( $z$ ) direction. The Reynolds number based on half channel height and friction velocity is  $Re_\tau = 180$ . The DNS employs a pseudospectral algorithm on a grid of size  $192 \times 128 \times 192$ , fully de-aliased in the  $x$  and  $z$  directions. Fluid and particle quantities are evolved with third-order Runge–Kutta time stepping, and a time step in wall units of  $\Delta t^+ = 0.2$ . Interpolation of quantities to particle locations is performed via the first derivative method (see Appendix B).

Fifteen ensembles of 500,000 particles each were evolved, comprising three modes of evolution (equilibrium Eulerian, modified equilibrium Eulerian, and exact Lagrangian) and five values of  $\tau_+$  ranging from 1 to 10 for each mode. The actual diameters of the particles depend on the density ratio  $\rho$ . Table 1 gives the particle diameter in wall units,  $d_p^+$ , corresponding to  $\rho = 1000$  for each  $\tau^+$  used in the simulation. Also shown in the table are the particle response times and diameters in Kolmogorov units, which are functions of wall-normal distance,  $y^+$ . The gravitational acceleration is zero in each case. The simulation was run to  $t^+ = 1000$ . Statistics were gathered at an interval of  $\Delta t^+ = 20$ , beginning at  $t^+ = 160$ . Thus, the particles were evolved for at least 16 response times before statistics were taken, allowing the particles to settle into a statistically steady state.

### 5.2. Results

The statistics on mean wall-normal slip velocity are shown in Fig. 6 for particles of size  $\tau^+ = 1$  and 3. These and all other quantities plotted for the turbulent channel flow are given in wall units, where the channel half height is the length scale and the friction velocity  $u^* = \sqrt{\tau_w/\rho_f}$  is the velocity scale. Here  $\tau_w$  is the wall shear stress and  $\rho_f$  is the fluid density. For the fluid the mean wall-normal velocity is constrained to be identically zero by continuity. In the absence of

Table 1

Response times and particle diameters (based on  $\rho = 1000$ ) in wall units, and in Kolmogorov units based on local conditions at  $y^+ = 30, 20,$  and  $7$

Size	$\tau^+$	$\tau^k _{30}$	$\tau^k _{20}$	$\tau^k _7$	$d_p^+$	$d_p^k _{30}$	$d_p^k _{20}$	$d_p^k _7$
I	1.00	0.269	0.323	0.342	0.134	0.0696	0.0762	0.0785
II	1.78	0.479	0.574	0.609	0.179	0.0929	0.1016	0.1047
III	3.16	0.852	1.021	1.083	0.239	0.1238	0.1355	0.1396
IV	5.62	1.515	1.815	1.926	0.318	0.1651	0.1807	0.1861
V	10.00	2.695	3.227	3.424	0.424	0.2202	0.2410	0.2482

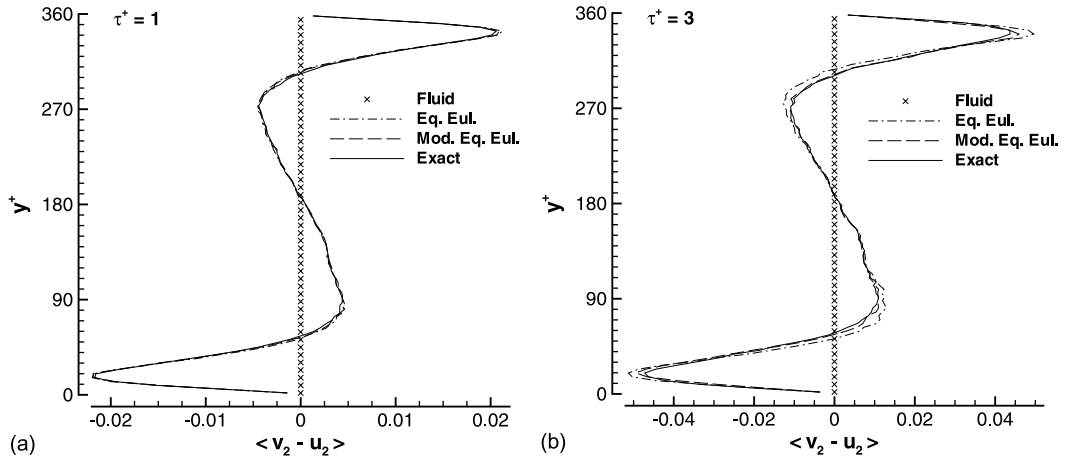


Fig. 6. Mean wall-normal relative velocity vs. distance from the wall: (a)  $\tau^+ = 1$  and (b)  $\tau^+ = 3$ .

gravitational settling, the nonzero wall-normal velocity for the particles seen in Fig. 6 is a clear indication of the turbophoretic effect. For the present case of particles much denser than the fluid the leading order behavior for the turbophoretic wall-normal velocity of the particles can be expressed as

$$\langle v_2 \rangle = -\tau^+ \frac{\partial}{\partial y^+} \langle u_2^2 \rangle. \tag{23}$$

Thus turbophoretic migration is down the gradient of rms wall-normal fluid velocity fluctuation. In the turbulent channel flow  $\langle u_2^2 \rangle$  reaches a local peak around  $y^+ \approx 60$ . Thus the denser-than-fluid particles on average move toward the wall in the near-wall region, but migrate toward the center of the channel away from the wall. For the smaller particle type, this behavior is accurately captured by both equilibrium approximations. Some differences begin to emerge for the larger particle type, where the improvement due to the locally implicit correction in the modified equilibrium approximation can be observed. Despite this slight improvement, it is clear that both the modified and unmodified methods are quite accurate in predicting turbophoretic migration.

The advantage of the locally implicit correction is quite evident in the mean streamwise slip velocity shown in Fig. 7. As a result of their turbophoretic migration the heavier-than-fluid particles on average lead the fluid close to the wall, but lag the fluid throughout the rest of the channel. This general trend is well captured by both equilibrium approximations. However, the magnitude of slip velocity is underpredicted by the unmodified equilibrium approximation and the underprediction is substantial for the larger particle type, resulting in more than 50% error. In contrast, the modified equilibrium approximation evaluates the streamwise slip velocity quite accurately.

A more complete picture can be obtained from the PDF of streamwise slip velocity. Fig. 8a shows the PDFs of  $v_1 - u_1$  for the various methods at  $y^+ = 7$  for  $\tau^+ = 1$ , which is where the error is the greatest. Note that for the approximation  $\mathbf{v} = \mathbf{u}$  the PDF of slip velocity is simply a Dirac delta function. Compared to this, both the modified and unmodified equilibrium Eulerian methods yield a much more realistic distribution. The unmodified method is in significant error

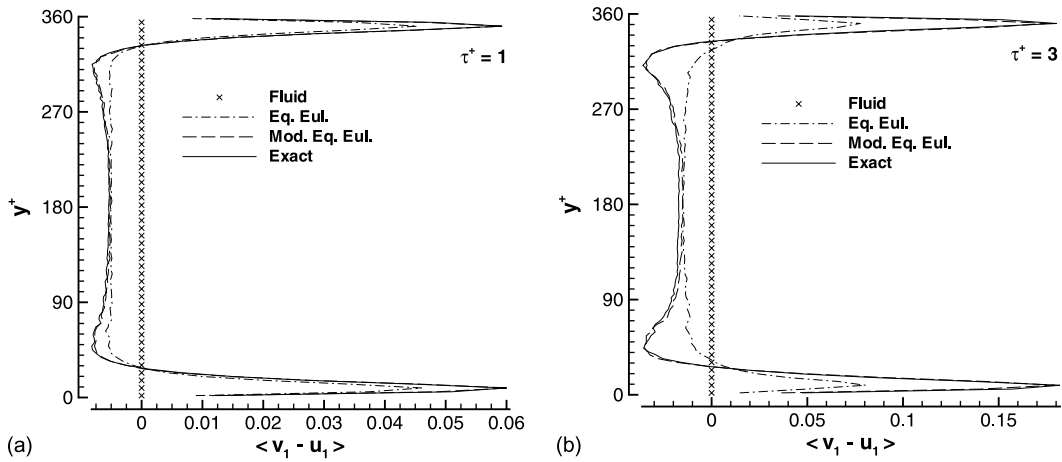


Fig. 7. Mean streamwise relative velocity vs. distance from the wall: (a)  $\tau^+ = 1$  and (b)  $\tau^+ = 3$ .

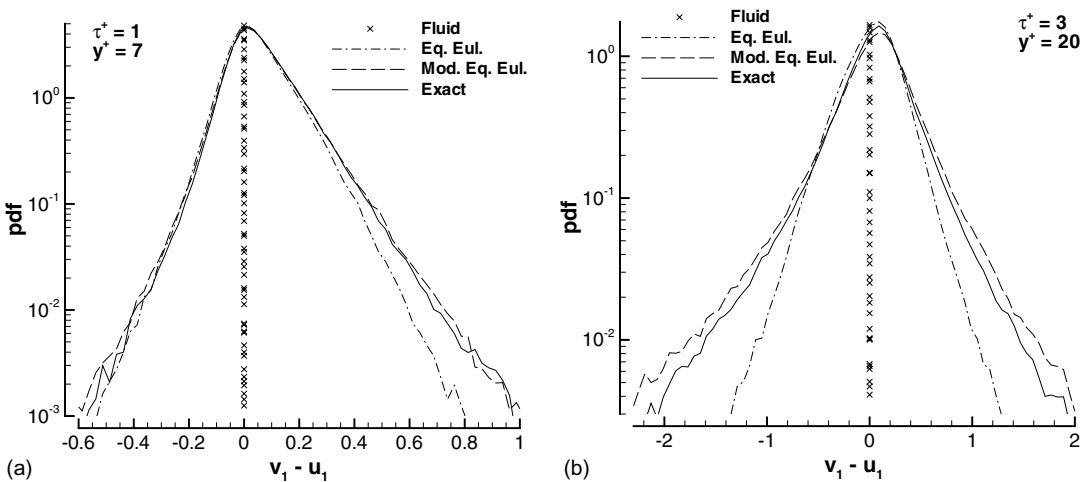


Fig. 8. PDFs of  $v_1 - u_1$ : (a)  $\tau^+ = 1$  and  $y^+ = 7$ , and (b)  $\tau^+ = 3$  and  $y^+ = 20$ .

only for the fastest moving particles which have migrated from the buffer region. The modified equilibrium approximation performs uniformly well. In the  $\tau^+ = 3$  case the PDFs are shown for  $y^+ = 20$ , which is more representative of the streamwise slip velocity PDFs over the bulk of the channel. In Fig. 8b the PDF for the exact particles shows an increased preference for a long tail with a larger number of very fast and slow moving particles compared to the local fluid. This behavior is well captured by the modified equilibrium approach, but has been underestimated in the unmodified case. Such a symmetric error does not adversely influence the statistics on mean streamwise slip velocity shown in Fig. 7, but does contribute to large errors in the higher even-order statistics.

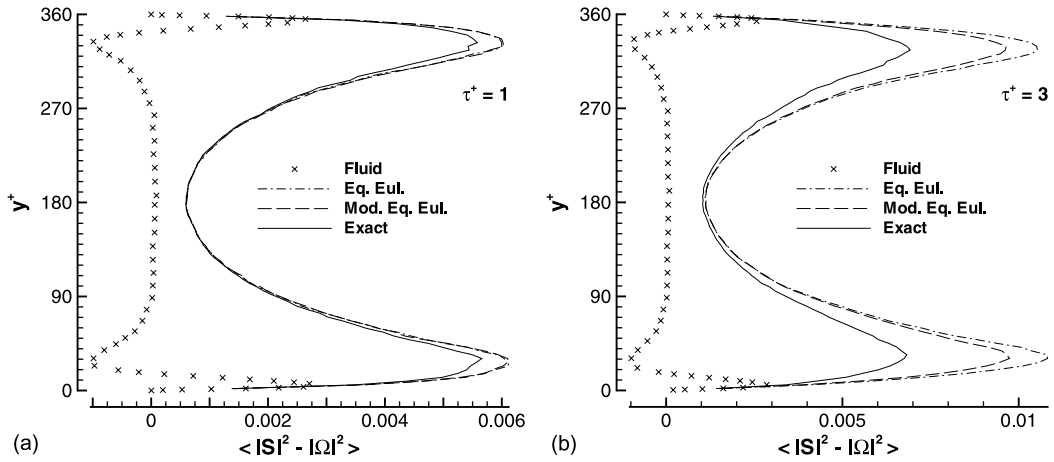


Fig. 9. Mean value of  $|\mathbf{S}|^2 - |\mathbf{\Omega}|^2$  vs. distance from the wall: (a)  $\tau^+ = 1$  and (b)  $\tau^+ = 3$ .

We will now address the statistics on preferential concentration with a plot of planar average of  $|\mathbf{S}|^2 - |\mathbf{\Omega}|^2$  in Fig. 9. The planar average of  $|\mathbf{S}|^2 - |\mathbf{\Omega}|^2$  for the fluid reaches a local minimum (large negative value) near  $y^+ = 30$  due to the predominance of vortical structures in the buffer layer. In contrast, when averaged over all particle positions,  $|\mathbf{S}|^2 - |\mathbf{\Omega}|^2$  reaches a strong positive peak in the buffer region. This difference in behavior is due to the inertia of the particles, which get spun out of vortices. The equilibrium approximations capture this tendency for preferential accumulation qualitatively; however, quantitative differences exist. The error in the equilibrium approximations is quite small for the smaller particles, but attains larger values as  $\tau^+$  increases. The locally implicit correction improves the statistics somewhat, but the error persists. This modest contribution from the modified equilibrium approximation in terms of preferential accumulation can be anticipated from the earlier results for a particle in a vortex.

The accuracy of the equilibrium approximations along with that of  $\mathbf{v} = \mathbf{u}$  is presented in Fig. 10 as the maximal deviation in  $\langle |\mathbf{S}|^2 - |\mathbf{\Omega}|^2 \rangle$  from that of the exact particles for varying  $\tau^+$ . The behavior of the modified and unmodified methods is similar for small  $\tau^+$ , whereas the modification mitigates the degree to which the equilibrium Eulerian method overestimates the preferential concentration for larger particles. This behavior is similar to the prediction made in Fig. 1 for the case of a vortex for large  $\eta$ .

We next look at the detailed distribution of  $|\mathbf{S}|^2 - |\mathbf{\Omega}|^2$ , limiting attention to the buffer region,  $y^+ = 30$ , where the error in the equilibrium approximation peaks. Fig. 11 plots the PDFs of  $|\mathbf{S}|^2 - |\mathbf{\Omega}|^2$  for both  $\tau^+ = 1$  and  $\tau^+ = 3$ . Compared to the fluid elements the behavior of the heavier-than-fluid particles is interesting: their avoidance of vortical regions is quite strong, but their tendency to congregate in regions of high strain is relatively mild. While this may be in agreement with the intuitive notion of particles being spun out of vortices, it is in contrast to the asymptotic result (22) of Maxey (1987), which states that dense particles avoid regions of high vorticity and seek regions of high strain-rate equally. This suggests that the particles with  $\tau^+ \geq 1$  are too large for the asymptotic result to accurately apply. Nevertheless, for  $\tau^+ = 1$  we observe that both the unmodified and the modified equilibrium approximations capture the entire PDF quite well.



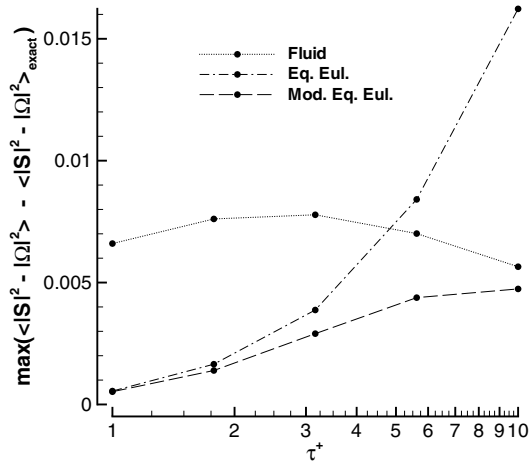


Fig. 10. Maximal discrepancies in  $\langle |S|^2 - |\Omega|^2 \rangle$  vs.  $\tau^+$ .

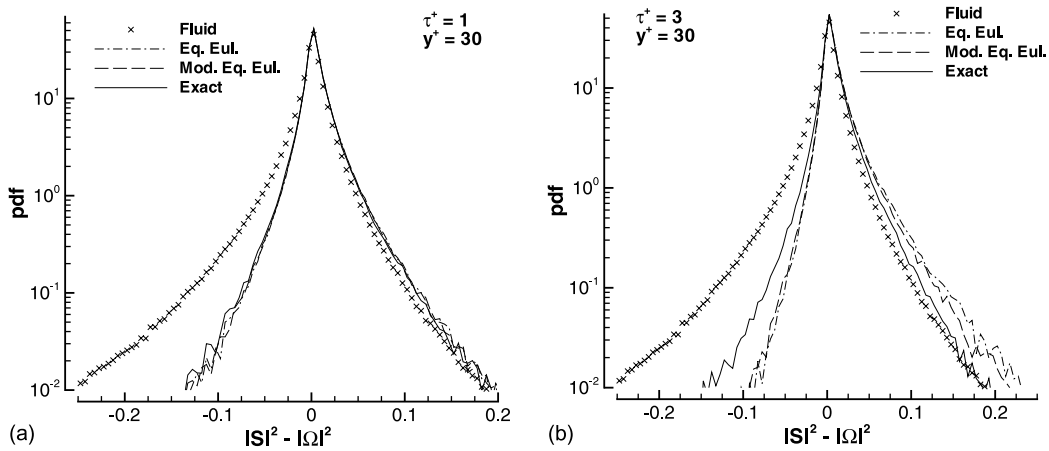


Fig. 11. PDFs of  $|S|^2 - |\Omega|^2$  at  $y^+ = 30$ : (a)  $\tau^+ = 1$  and (b)  $\tau^+ = 3$ .

For  $\tau^+ = 3$ , the PDF is predicted by both equilibrium approximations to only reasonable accuracy. The overprediction of large positive values and the corresponding underprediction of large negative values is responsible for the exaggerated mean preferential concentration observed in Fig. 9b. As can be expected, the PDF of the modified equilibrium approximation is in somewhat better agreement with that of the exact particles.

Finally, through direct observation of the particle distribution we will demonstrate that in spite of the increase in preferential concentration for the large particles, their distribution remains physically meaningful and provides a good approximation to the distribution of exact particles. Fig. 12 shows scatter plots of all  $\tau^+ = 3$  particles at  $t^+ = 200$  within a narrow slice about  $y^+ = 30$ . The exact particles are in the middle, for comparison with the unmodified equilibrium Eulerian (top) and modified equilibrium (bottom) particles. Both the unmodified and modified are quite

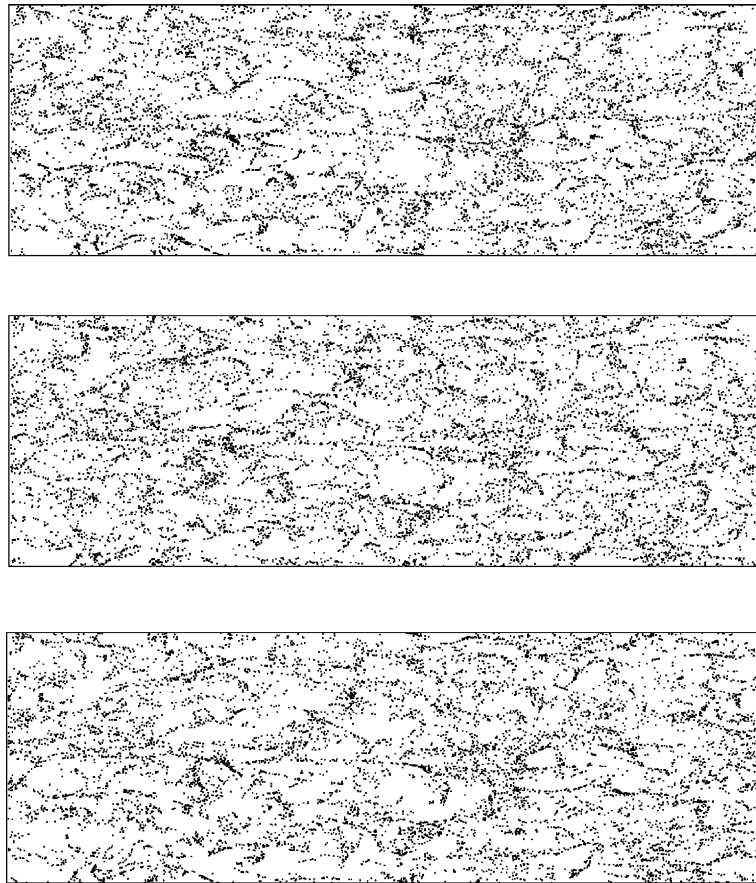


Fig. 12. Equilibrium Eulerian, exact, and modified equilibrium Eulerian particles:  $\tau^+ = 3$ ,  $t^+ = 200$ ,  $y^+ = 30$ .

similar in appearance to the exact case, even for this worst-case location. The reason for this is that the change in the mean value is caused by an exaggerated abhorrence of the regions of strongest gradient, whereas the distribution of the majority of the particles is represented quite accurately, a result which was illustrated by the PDFs. For the modified equilibrium Eulerian the exaggerated abhorrence of the strong gradient regions is diminished somewhat, so the bottom scatter plot should approximate the middle one somewhat better. The qualitative agreement is rather impressive when one compares it to the alternative of using  $\mathbf{v} = \mathbf{u}$ , which would give a statistically uniform distribution of particles for all time.

## 6. Conclusions

Small particles in a fluid follow the flow closely, but not exactly. The difference between the particle and fluid velocities causes particles to accumulate preferentially, and therefore must be taken into account. The Eulerian–Eulerian method is one way of doing this, but it requires solving

a system of PDEs for the particle velocity field. Ferry and Balachandar (2001) have shown that, in the dilute regime, sufficiently small particles entrain exponentially fast to a unique equilibrium velocity field. Based on this idea, the equilibrium Eulerian method for multiphase flow has been developed. This method uses a first-order approximation (in particle response time  $\tau$ ) to the equilibrium velocity in order to approximate the exact velocity. The method performs well for small particles, but begins to exhibit certain errors as  $\tau$  increases. In particular, it fails to represent the fact that particles migrating through a shear layer remember the velocity of the previous layer for a period of time.

The present work defines a modified equilibrium Eulerian method with the closure  $d\mathbf{v}/dt \approx d\mathbf{u}/dt$ . Although still approximate, this closure retains the physics associated with the convective derivative  $\mathbf{v} \cdot \nabla$ , which represents the change in fluid conditions along the direction of particle motion. This improved closure results in the modified equilibrium approximation (5). The modified equilibrium approximation requires the inversion of a  $3 \times 3$  matrix locally at every point in the flow and therefore is somewhat more involved than the unmodified equilibrium approximation. However, both equilibrium approximations are computationally far simpler than the standard Eulerian approach, which requires solving additional PDEs. The equilibrium approximations are then tested for a variety of linear flows. Despite the simplicity of these flows, it is quite illuminating to compare the exact results for particles versus those for particles evolving under the approximate velocities given by the unmodified and modified equilibrium methods.

In a shear flow the unmodified method exhibits a streamwise velocity equal to that of the local fluid, whereas the modified method accounts accurately for the memory the particle retains as it crosses fluid streamlines. Similar behavior was observed in the case of radial migration of particles in a vortical flow. For small particles there is excellent agreement ( $O(\tau^3)$  error) between the exact, modified, and unmodified methods. For moderate sized particles, there is some disagreement between the exact result and the unmodified equilibrium approximation. The locally implicit correction improves the prediction by only about 20%.

Along the direction of extensional strain for small particles there is good agreement ( $O(\tau^2)$  error) between the exact, modified, and unmodified methods. For moderate sized particles, there is some disagreement between the exact result and the unmodified equilibrium approximation. The locally implicit correction provides substantial (50%) improvement to the prediction. Along the direction of compressional strain for small particles there is good agreement ( $O(\tau^2)$  error) between the exact, modified, and unmodified methods. For moderate sized particles, owing to their oscillatory behavior, there is no unique representation for the exact velocity in terms of position. Nevertheless, the equilibrium methods continue to provide a reasonable approximation to the average behavior.

The performance of the equilibrium approximations was first evaluated in a DNS of isotropic turbulence. Preferential concentration was assessed in terms of the statistics of  $|\mathbf{S}|^2 - |\mathbf{\Omega}|^2$  and of swirling strength. In each case, a maximal mean value for the exact particles occurs for  $\tau^k = 0.64$ . The unmodified equilibrium Eulerian method indicates an ever-increasing preferential concentration, with increasing  $\tau^k$ . The modified method, on the other hand, recovers the correct behavior, with the peak mean value at  $\tau^k \approx 1$ .

A DNS of turbulent channel flow was performed to compare the evolution of discrete particles following the unmodified and modified equilibrium Eulerian velocities to particles following the exact Lagrangian velocity. There is very little error in the wall-normal relative velocity for  $\tau^+ \lesssim 3$

(corresponding to  $\tau^k \lesssim 1$ ) even with the unmodified method. For the statistics of streamwise relative velocity, the unmodified method begins to perform poorly for  $\tau^+ \geq 1$ : it fails to account for the particles' memory of their higher streamwise velocity as they migrate toward the wall. The modified method accounts for this effect, as expected based on the result for the shear flow and vortex examples. The degree of preferential concentration is assessed by computing  $|\mathbf{S}|^2 - |\mathbf{\Omega}|^2$ . Both the unmodified and modified methods yield fairly accurate PDF statistics of  $|\mathbf{S}|^2 - |\mathbf{\Omega}|^2$ .

All the results presented have been for the limit of dense particles ( $\rho \gg 1$ ). The modified equilibrium Eulerian method applies equally well for light particles or (sufficiently rigid) bubbles. In this case, added mass, pressure gradient, and Faxén terms must be retained in the Maxey–Riley equation (Maxey and Riley, 1983):

$$\rho \frac{d\mathbf{v}}{dt} = \frac{\mathbf{u} - \mathbf{v}}{\tau_0} + \frac{D\mathbf{u}}{Dt} + C_M \left( \frac{D\mathbf{u}}{Dt} - \frac{d\mathbf{v}}{dt} \right) + (\rho - 1)\mathbf{g} + \frac{3v}{4} \Delta\mathbf{u}, \quad (24)$$

where  $\tau_0 = \tau/\rho = d^2/(18\nu)$ , and  $C_M$  is the added mass coefficient ( $C_M = 1/2$  for spherical particles). Applying the closure  $d\mathbf{v}/dt \approx d\mathbf{u}/dt$ , as was done to obtain (4), yields

$$\mathbf{v}_m = \mathbf{u} + \tau_0 \frac{3v}{4} \Delta\mathbf{u} - (\rho - 1)\tau_0 (\mathbf{I} + (\rho + C_M)\tau_0 \mathbf{G})^{-1} \left( \frac{D\mathbf{u}}{Dt} - \mathbf{g} \right). \quad (25)$$

The unmodified method has been validated for bubbles (Ferry and Balachandar, 2001), and it was found that the method performs equally well for different values of  $\rho$  when comparing particle types with equal values of  $|(\rho - 1)\tau_0|$  under the same conditions. The same may be said of the modified method. The modified method can also be used with a value of  $\tau$  that accounts empirically for nonlinear drag, just as the unmodified method can (Ferry and Balachandar, 2002).

## Appendix A. Avoiding singularities

The modified equilibrium Eulerian method can produce anomalously large values of velocity when the matrix  $\mathbf{I} + \tau\mathbf{G}$  approaches singularity. This occurs when an eigenvalue of  $\mathbf{G}$  approaches the value  $-1/\tau$ , corresponding to a region of intense compressive strain. In practice this is usually not a problem because of the requirement that  $\tau$  be small enough for the equilibrium approach to be applicable. Therefore, over most of the flow's domain, we anticipate the locally implicit correction to be applied without any difficulty. However, there may exist small regions of intense compressive strain where there are difficulties. A simple way to deal with the possible singularity of  $\mathbf{I} + \tau\mathbf{G}$  is to determine whether the matrix is nearly singular, and to replace the resulting, extremely large value of  $\mathbf{v}_m$  with some reasonable value. (Note that for such strong compressional strain there is no unique equilibrium particle velocity in any case.) However, this simple procedure produces a field  $\mathbf{v}_m$  which is not smooth.

Instead, we modify (5) to contain an adjustable parameter  $\alpha$ :

$$\mathbf{v}_m = \mathbf{u} - \tau(\mathbf{I} + \alpha\tau\mathbf{G})^{-1} \left( \frac{D\mathbf{u}}{Dt} - \mathbf{g} \right). \quad (\text{A.1})$$

When  $\alpha = 1$ , the modified method is obtained; when  $\alpha = 0$ , the unmodified method. For intermediate values of  $\alpha$ , Eq. (A.1) can be viewed as an interpolation between the modified and unmodified methods.

The value of  $\alpha$  is chosen to ensure the invertibility of  $\mathbf{I} + \alpha\tau\mathbf{G}$ . The procedure we use has two virtues: (a) it avoids any explicit calculation of eigenvalues, and (b) it produces a value of  $\mathbf{v}_m$  that varies smoothly with  $\mathbf{G}$ . The latter property is important because when  $\mathbf{v}_m$  is used to evolve a particle concentration field it is necessary to take its spatial derivatives.

To compute  $\alpha$ , let  $G_2$  and  $G_3$  be the second and third invariants of  $\mathbf{G}$ :

$$G_2 = \begin{vmatrix} g_{22} & g_{23} \\ g_{32} & g_{33} \end{vmatrix} + \begin{vmatrix} g_{33} & g_{31} \\ g_{13} & g_{11} \end{vmatrix} + \begin{vmatrix} g_{11} & g_{12} \\ g_{21} & g_{22} \end{vmatrix}, \quad G_3 = \det(\mathbf{G}). \tag{A.2}$$

Now define  $\chi$  as

$$\chi = \tau \left( 8 \max(0, -G_2)^3 + 8 \max(0, -G_3)^2 \right)^{1/6}, \tag{A.3}$$

and let

$$\alpha = \begin{cases} 1, & \text{if } \chi \leq 1, \\ 0, & \text{if } \chi \geq 2, \\ (1 - \cos(\pi\chi))/2, & \text{otherwise.} \end{cases} \tag{A.4}$$

This procedure guarantees that  $\det(\mathbf{I} + \alpha\tau\mathbf{G}) > 0.207$ .

Fig. 13, re-plots Fig. 2 with the procedure to avoid singularity. The extensional strain case is affected as well because it is assumed to be part of a divergence-free flow. (To avoid this, one could employ a correction that acts only on the eigenspace for the compressive eigenvalue). The vortical and shear cases are unaffected. Fig. 14 shows the fraction of particles for which  $\alpha = 1$  at all distances  $y^+$  from the wall for  $\tau^+ = 3$  particles. It is clear that the singularity correction is needed for less than 1% of particles even at  $y^+ = 30$ . In the isotropic turbulence case,  $\alpha = 1$  for all  $\tau^k = 1.28$  particles.

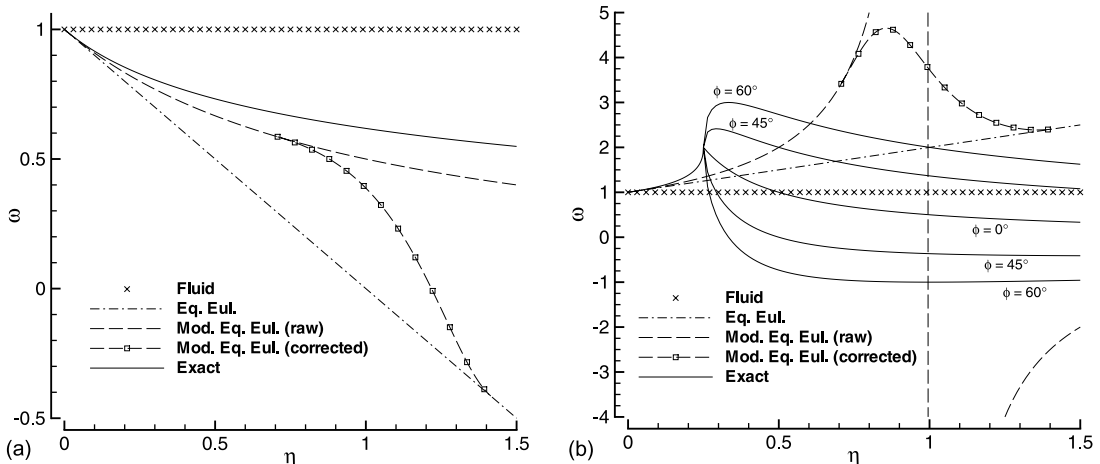


Fig. 13. Velocity factors for (a) extensional and (b) compressive strain.

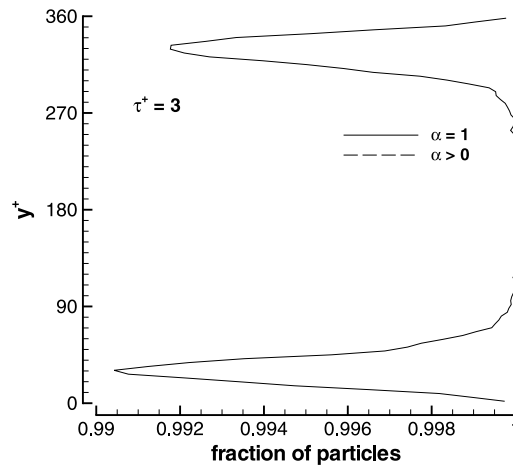


Fig. 14. Fraction of particles without correction vs. distance from the wall for  $\tau^+ = 3$ .

## Appendix B. Interpolation scheme

We introduce a new method which has the same accuracy as shape function method (SFM) at high wave numbers (Balachandar and Maxey, 1989), but has fourth-order accuracy overall. The method is as fast as SFM, and makes better (optimal) use of the same derivative information. SFM assumes the mixed derivatives to be zero, whereas the new method estimates these derivatives as effectively as possible given the information it has.

Let  $\Delta x = x_1 - x_0$ ,  $x = (x - x_0)/\Delta x$ , with similar definitions for the  $y$  and  $z$  directions. Then define the following basis functions:

$$\begin{aligned} L_0(x) &= (1 - x), & L_1(x) &= x, \\ M_0(x) &= (1 - 2x)x, & M_1(x) &= (2x - 1)(1 - x), \\ N_0(x) &= x(1 - x), & N_1(x) &= -x(1 - x). \end{aligned} \quad (\text{B.1})$$

Given  $x_0 \leq x \leq x_1$ ,  $y_0 \leq y \leq y_1$ , and  $z_0 \leq z \leq z_1$ , an interpolated quantity  $\tilde{u}(x, y, z)$  is calculated thusly:

$$\begin{aligned} \tilde{u}(x, y, z) &= \sum_{i=0}^1 \sum_{j=0}^1 \sum_{k=0}^1 L_i(x)L_j(y)L_k(z) \left( (1 + M_i(x) + M_j(y) + M_k(z))u(x_i, y_j, z_k) \right. \\ &\quad \left. + N_i(x)u_x(x_i, y_j, z_k) \Delta x + N_j(y)u_y(x_i, y_j, z_k) \Delta y + N_k(z)u_z(x_i, y_j, z_k) \Delta z \right). \end{aligned} \quad (\text{B.2})$$

Because of its optimal usage of first-derivative information, this interpolation scheme is termed the first derivative method.

## References

- Balachandar, S., Maxey, M.R., 1989. Methods for evaluating fluid velocities in spectral simulations of turbulence. *Journal of Computational Physics* 83, 96–125.

- Brooke, J.W., Hanratty, T.J., McLaughlin, J.B., 1994. Free-flight mixing and deposition of aerosols. *Phys. Fluids* 6, 3404–3415.
- Camparaloni, M., Tampieri, F., Trombetti, F., Vittori, O., 1975. Transfer of particles in nonisotropic air turbulence. *Journal of Atmospheric Science* 32, 565.
- Eaton, J.K., Fessler, J.R., 1994. Preferential concentration of particles by turbulence. *Int. J. Multiphase Flow* 20 (suppl.), 169–209.
- Eswaran, V., Pope, S.B., 1988a. An examination of forcing in direct numerical simulations of turbulence. *Computers and Fluids* 16, 257–278.
- Eswaran, V., Pope, S.B., 1988b. Direct simulations of the turbulent mixing of a passive scalar. *Phys. Fluids* 31, 506–520.
- Ferry, J., Balachandar, S., 2001. A fast Eulerian method for disperse two-phase flow. *Int. J. Multiphase Flow* 27, 1199–1226.
- Ferry, J., Balachandar, S., 2002. Equilibrium expansion for the Eulerian velocity of small particles. *Powder Technology* 125, 131–139.
- Friedlander, S.K., Johnstone, H.F., 1957. Deposition of suspended particles from turbulent gas streams. *Industrial and Engineering Chemistry* 49, 1151–1156.
- Kallio, G.A., Reeks, M.W., 1989. A numerical simulation of particle deposition in turbulent boundary layers. *Int. J. Multiphase Flow* 15, 433–446.
- Manninen, M., Taivassalo, V., Kallio, S., 1996. On the mixture model for multiphase flow. Technical Report 288, VTT publications, Technical Research of Finland, Espoo.
- Marble, F.E., 1970. Dynamics of dusty gases. *Annual Review of Fluid Mechanics* 2, 397–446.
- Maxey, M.R., 1987. The gravitational settling of aerosol particles in homogeneous turbulence and random flow fields. *J. Fluid Mech.* 174, 441–465.
- Maxey, M.R., Riley, J.J., 1983. Equation of motion for a small rigid sphere in a nonuniform flow. *Phys. Fluids* 26, 883–889.
- Reeks, M.W., 1983. The transport of discrete particles in inhomogeneous turbulence. *Journal of Aerosol Science* 14, 729–739.
- Saffman, P.G., 1962. On the stability of laminar flow of a dusty gas. *J. Fluid Mech.* 13, 120–128.
- Squires, K.D., Eaton, J.K., 1991. Preferential concentration of particles by turbulence. *Phys. Fluids A* 3, 1169–1178.
- Zhou, J., Adrian, R.J., Balachandar, S., 1996. Autogeneration of near-wall vortical structures in channel flow. *Phys. Fluids* 8, 288–290.